Environ. Sci. Technol. **2003**, *37,* 3392−3398

Modelling Binary Homogeneous Nucleation of Water−Sulfuric Acid Vapours: Parameterisation for High Temperature Emissions

H. VEHKAMÄKI,* M. KULMALA, AND K. E. J. LEHTINEN

Division of Atmospheric Sciences, Department of Physical Sciences, P.O. Box 64 (Gustaf Hällströmin katu 2) FIN-00014 University of Helsinki, Finland

M. NOPPEL

Institute of Environmental Physics, University of Tartu, 18 Ülikooli Str., 50090, Tartu, Estonia

Particles formed in the automobile exhaust might form a significant fraction of fine particles in urban air. We have developed a model and produced parametrizations for predicting the particle formation rate at exhaust conditions. We studied the formation in the mixture of water and sulfuric acid vapors and at temperatures between 300 and 400 K. A thermodynamically consistent version of the classical binary homogeneous nucleation model was used. The needed thermodynamical input data (vapor pressures, chemical activities, surface tensions, densities) are carefully investigated and utilized in thermodynamically consistent way. The obtained nucleation rates are parametrized in order to be able to use this nucleation model in aerosol dynamic models, exhaust models, or other process models. The parametrization reduces computational time at least by a factor of 500.

1. Introduction

Fine particles, and in particular vehicle related exhaust aerosol, have lately received increasing attention by the scientific community as well as health organizations. This is due to evidence which has linked adverse health effects to urban ultrafine aerosol populations (*1*). Epidemiological studies have, for example, linked ambient particle matter with mortality rates, hospital admissions, and respiratory symptoms (*2*). Vehicle aerosol emissions are under inspection for carcinogenic and noncarcinogenic health effects (*3*, *4*). Thus it is very important to both experimentally and theoretically investigate the pathways of particle formation and growth in engine exhaust. The capability of predicting formation rates of new particles with different fuel and driving conditions, etc. relies on understanding the nucleation mechanisms and rates of the process at hand.

Shi and Harrison (*5*) investigated ultrafine particle formation during diesel exhaust dilution experimentally and theoretically. They found that by using the parametrization for binary water−sulfuric acid nucleation, including the effect of hydration, by Kulmala et al. (*6*), the qualitative agreement between theory and experiments was reasonable, but the maximum nucleation rate predicted by theory was much too low. They concluded that biogenic species, possibly ammonia, contribute to the nucleation process and also increase its rate significantly. Similar studies were conducted by Abdul-Khalek et al. (*7*, *8*). They used a modern medium-duty diesel engine and various different dilution conditions to find out nucleation and condensational growth rates. By comparing the results to a simple theoretical assessment, utilizing again a parametrization for binary water−sulfuric acid nucleation and condensational growth equations, they concluded that the nucleation mechanism can explain the formation of new particles. However, the observed growth rates were much too high to be explained by the available sulfuric acid amounts. The discrepancy was explained by condensable hydrocarbons. These conclusions were later confirmed by analyzing the chemical composition of diesel nanoparticles using a nano-DMA with thermal desorption particle beam mass spectrometry (*9*). Similar particle formation mechanisms have been identified for example in ambient air (*10*), in the tropical marine boundary layer (*11*), in boreal forests (*12*).

One problem with all the studies mentioned above is the use of nucleation parametrizations based on atmospheric conditions, and their possible extrapolation to much higher temperatures involved in diesel exhausts. This brings up the main motivation of this paper—to develop a new nucleation model and parametrizations for binary water−sulfuric acid nucleation, the validity of which extends to the conditions of interest. Whereas our much used previous parametrization (*6*) covers the temperature range 233−298 K, the present parametrization will cover the range 300−400 K. Even if it is likely that nucleation at high temperatures, e.g. associated with diesel engine exhaust dilution, involves additional species than just water and sulfuric acid, we believe that such an extension of the present models is very useful, even if only to rule out the binary mechanism.

The main aim of this paper is to investigate binary nucleation mechanism of water−sulfuric acid system at temperatures higher than room temperature. We present a parametrization for the water−sulfuric acid nucleation that is valid for the engine exhaust dilution conditions.

2. Theory and Model

Here we will give only a brief overview of the classical nucleation theory. For a more detailed description the reader is referred to our earlier work (*6*, *13*) and references therein.

Nucleation is the formation of supercritical stable clusters. A critical cluster can be identified by finding the maximum of the formation free energy with respect to number of water and acid molecules. The critical cluster composition can be solved from the equation

$$\frac{1}{v_a(x^*)}\ln\frac{\rho_a^{free}}{\rho_{a,s}^{free}(x^*)}=\frac{1}{v_w(x^*)}\ln\frac{\rho_w^{free}}{\rho_{w,s}^{free}(x^*)}, \qquad (1)$$

where v_a and v_w are the composition dependent partial molar volumes of acid and water, respectively. ρ_i^{free} is the number concentration of free molecules of component i in the nucleating vapor and $\rho_{i,s}^{free}(x)$ is the number concentration of component i in saturated vapor above a solution with sulfuric acid mole fraction x. The asterisk refers to the critical cluster.

Chemical ion mass spectroscopy (*14*), diffusion studies (*15*), and ab initio calculations (*16*) indicate that sulfuric acid tends to form hydrates in the vapor phase. These small clusters of acid and water molecules have negative formation energy, and they stabilize the vapor and hinder nucleation.

* Corresponding author phone: +358-9-191 50710; fax: +358-9-50717; e-mail: Hanna.Vehkamaki@helsinki.fi.

10.1021/es0263442 CCC: $25.00
Published on Web 06/28/2003

In nucleation experiments the total concentration of sulfuric acid molecules (containing also the acid molecules bound in hydrates) is measured, but the concentration of free acid molecules (not bound to hydrates) enters the nucleation energetics (e.g. via eq 1). The number concentrations of i-hydrates $\rho(1, i)$ are given by (*17*)

$$\rho(1, i) = K_1 \cdot K_2 \ldots \cdot K_i \left(\frac{\rho_w^{free}}{\rho_0}\right)^i \rho_a^{free}, \quad (2)$$

and the ratio of the total acid concentration to the number concentration of free acid molecules in the gas phase is (*18, 19*)

$$\frac{\rho_a^{total}}{\rho_a^{free}} = 1 + K_1 \frac{\rho_w^{free}}{\rho_0} + \cdots + K_1 \cdot K_2 \ldots \cdot K_i \left(\frac{\rho_w^{free}}{\rho_0}\right)^i + \cdots + K_1 \cdot K_2 \ldots \cdot K_N \left(\frac{\rho_w^{free}}{\rho_0}\right)^N \quad (3)$$

Here N is the number of water molecules in the largest hydrate taken into account, and K_i are the equilibrium constants for successive additions of water molecules to an acid molecule. Their temperature-dependent values are given by Noppel at al. (*13*). The extent of hydration is predominantly determined by equilibrium constants K_1 and K_2 which are obtained by fitting to the result of ab initio calculations and experimental data related to hydrates. Classical theory is only used to estimate the minor effect of hydrates with 3−5 water molecules. The equilibrium constants are calculated at a reference vapor concentration $\rho_0 = p_0/(kT)$ with a reference pressure p_0 set to 1 atm. We assume that the concentrations of hydrates with more than one acid molecule are negligible and that the concentration of water vapor is not significantly affected by the hydrate formation ($\rho_w^{free} = \rho_w^{total}$).

The radius of the critical cluster is given by the Kelvin equation

$$r^* = \frac{2\sigma(x^*)v_i(x^*)}{kT \ln(\rho_i^{free}/\rho_{i,s}^{free}(x^*))}, \quad (4)$$

where σ is the surface tension of the solution, k is the Boltzmann constant, and T is the temperature. Equation 1 ensures that the value of r^* is independent of the choice of the component i = a, w. The work of formation for the critical nucleus is

$$W^* = \frac{4}{3}\pi r^{*2}\sigma(x^*) \quad (5)$$

and the general expression for nucleation rate J is (*20, 21*)

$$J = Z \cdot \rho(1, 2) \cdot \exp\left[\frac{-(W^* - W(1, 2))}{kT}\right] \quad (6)$$

where $W(1, 2)$ is the formation energy of the sulfuric acid dihydrate given by the classical theory and $\rho(1, 2)$ is the number concentrations of dihydrates given by eq 2. Z is a kinetic prefactor, and the product of the two last terms is the equilibrium concentration of critical nuclei (*13*). Here we use the dihydrate (one sulfuric acid bound to two water molecules) as a reference size. The cluster size distribution has been set to give $\rho(1, 2)$ for the number concentrations of dihydrates. The classical size distribution of clusters is not uniquely defined (*22*), but we can avoid the arbitrariness by using a reference size whose formation energy and concentration is known from experiments and/or ab initio calculations. We chose the dihydrate as a reference size since it is the largest (and thus closest to the critical size) water−sulfuric acid cluster extensively studied with ab initio methods.

3. Thermodynamics

To solve the composition and the radius of the critical cluster and subsequently to calculate the nucleation rate we need to know the surface tension and density of the solution as well as the equilibrium vapor pressures of sulfuric acid and water above a flat surface of the solution. For pure water we use the saturation vapor pressure (Nm^{-2}, T in K) according to Preining et al. (*23*)

$$p_w = \exp\{77.34491296 - 7235.424651/T - 8.2 \ln T + 5.7113 \cdot 10^{-3} T\} \quad (7)$$

and for sulfuric acid vapor pressure (Nm^{-2}, T in K) we use the formula based on the work of Ayers et al. (*24*), which is corrected for lower temperatures by Kulmala and Laaksonen (*25*):

$$p_a = 101325 \exp\left\{L + 10156\left[\frac{1}{360.15} - \frac{1}{T} + \frac{0.38}{545}\left(1 + \ln\left(\frac{360.15}{T}\right) - \frac{360.15}{T}\right)\right]\right\} \quad (8)$$

The value of the parameter $L = -11.695$ was fitted to various experimental and ab initio data in our recent paper (*13*).

We fitted a simple power function to the experimental surface tension data of Sabinina and Terpugow, Morgan and Davies, Suggitt et al., Hoffmann and Seeman, and Myhre et al. (*26−30*) in the temperature range 233−323 K. This function fits very well the experimental data of pure water (*31*). The experimental data points of Myhre et al. (*30*) with sulfuric acid mass fraction 0.291 deviate from the trend of other points, and they were not used in the fitting.

To establish a sounder basis for the extrapolation of the surface tension fit to temperatures higher than 323 K we have required that the surface tensions goes to zero at the critical temperature, as it physically should.

The following fit gives the surface tension σ (J/m^2) for all sulfuric acid mole fractions x where the solution is liquid:

$$\sigma(x, T) = (a + bT_1)T_1^{1.256}$$

$$T_1(x, T) = 1 - \frac{T}{T_c}$$

$$a(x) = 0.2358 - 0.529x + 4.073x^2 - 12.6707x^3 + 15.3552x^4 - 6.3138x^5$$

$$b(x) = -0.14738 + 0.6253x - 5.4808x^2 + 17.2366x^3 - 21.0487x^4 + 8.719x^5$$

The pseudocritical temperature of binary solution $T_c(x)$

$$T_c(x) = 647.15(1 - x)^2 + 900.0x^2 + 3156.186x(1 - x) \quad (9)$$

was estimated using the mixing rule (*32*) where the value 647.15 stands for the critical temperature of pure water (in Kelvin) (*31*), 900 stands for the critical temperature of pure sulfuric acid (in Kelvin) taken from Tables 3−10 in Reid et al. (*32*), and binary parameter 3156.186 was estimated by fitting. Figure 1 shows that eq 9 reproduces the experimental surface tension data well, and the extrapolation to higher temperatures behaves smoothly.

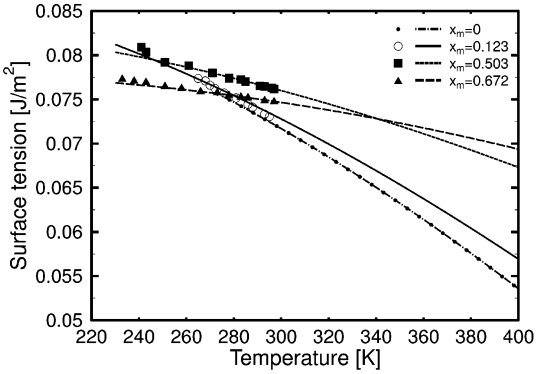

FIGURE 1. Comparison between the surface tension parametrization (lines) and the experimental surface tension data of (symbols). Different lines types and symbols represent different mass fractions x_m of sulfuric acid in the liquid.

In our earlier paper (*33*) we presented a polynomial function fitted to the density data for the sulfuric acid solution at 273−373 K from the *International Critical Tables* [1928] (*34*).

Activity coefficients for the water−sulfuric acid solution are crucial parameters in the nucleation calculations (*35*, *36*). The most rigorous method for evaluating the activity coefficients has been presented by Clegg et al. (*36*, *37*). It includes ionic solutes and gives the measured thermodynamic properties quite accurately. However, from a computational point of view, it is slow and valid only up to a sulfuric acid mole fraction of 0.42. In a recent study (*13*) we have compared the thermodynamic model of Clegg et al. (*37*, *36*) with the liquid-phase activity model of Zeleznik (*38*). We have shown that the resulting hydrate distributions and nucleation rates do not differ significantly. For our nucleation model we will use the activity coefficients by Zeleznik (*38*) because their formulation saves computer time and they are valid also at high sulfuric acid concentrations found in critical nuclei and higher temperatures (recommended temperature range up to 350 K).

4. Results and Discussion

The developed model has been used to account for nucleation rates under different conditions. Several thousand model runs have been performed in order to produce well established parametrizations for nucleation rates and cluster properties. The underlying classical nucleation theory has well known weaknesses since it is relying on using bulk liquid properties for small clusters. It is however at present the only model applicable to nucleation in nonideal, atmospherically relevant vapor mixtures. We have used experimental data and ab initio results where available to improve the classical model.

4.1. Parametrizations. The present parametrization is valid for the temperature range 300.15−400.15 K, relative humidities 1−100%, and total sulfuric acid concentrations $2\cdot10^9$−$5\cdot10^{15}$ /cm^3. However, we should remember that strictly speaking experimental results for surface tension exist only when T < 323 K, for density when T < 373 K, and for activities T < 350 K. At temperatures above these we have used extrapolations. However, the nucleation rate does not depend significantly on the surface tension and density formulas used. As a sensitivity analysis we compared the nucleation rates obtained using our formulas to rates calculated using the formulas given by Myhre et al. (*30*), and difference in nucleation rates was at most 1 order of magnitude, in most cases just 10−20%.

The fit is only valid in a region where it produces a nucleation rate in the range 10^{-1}−10^{14} 1/(cm^{3}s), the mole fraction of sulfuric acid in the critical cluster given by eq 10 is greater than 0.15 and the total number of molecules in the critical cluster given by eq 12 is at least 4. Also the cases where the critical cluster would be a hydrate (clusters with one sulfuric acid and 1−5 water molecules) are excluded from the region of validity. Note that when using the fit for the nucleation rate it is important to use also eqs 10 and 12 to check that these restrictions on cluster size are not violated.

The mole fraction of sulfuric acid in the critical cluster is given by

$$x^* = 0.847012 - 0.0029656\,T - 0.00662266\ln(N_a) + 0.0000587835\,T\ln(N_a) + 0.0592653\ln\left(\frac{RH}{100}\right) - 0.000363192\,T\ln\left(\frac{RH}{100}\right) + 0.0230074\ln\left(\frac{RH}{100}\right)^2 - 0.0000851374\,T\ln\left(\frac{RH}{100}\right)^2 + 0.00217417\ln\left(\frac{RH}{100}\right)^3 - 7.923\cdot10^{-6}\,T\ln\left(\frac{RH}{100}\right)^3 \quad (10)$$

where N_a is the total gas-phase concentration of sulfuric acid (1/cm^3), T is the absolute temperature, and RH is the relative humidity in percent.

The nucleation rate is given by an exponential of a third-order polynomial of ln(RH/100) and ln(N_a)

$$J[1/(cm^3 s)] = \exp[a(T, x^*) + b(T, x^*)\ln(RH/100) + c(T, x^*)\ln(RH/100)^2 + d(T, x^*)\ln(RH/100)^3 + e(T, x^*)\ln(N_a) + f(T, x^*)\ln(RH/100)\ln(N_a) + g(T, x^*)\ln(RH/100)^2\ln(N_a) + h(T, x^*)\ln(N_a)^2 + i(T, x^*)\ln(RH/100)\ln(N_a)^2 + j(T, x^*)\ln(N_a)^3] \quad (11)$$

where the coefficients $a(T, x^*)$...$i(T, x^*)$ are functions of temperature and critical cluster mole fraction x^* (calculated using eq 10):

$$a(T, x^*) = -0.00156975 - 0.134245\,T + 0.100507\,T^2 - 0.000460103\,T^3 + \frac{0.187416}{x^{*2}} + \frac{0.0104122}{x^*}$$

$$b(T, x^*) = 0.00195077 + 0.168038\,T - 0.0225755\,T^2 + 0.0000827149\,T^3 + \frac{0.0025029}{x^{*2}} + \frac{0.0155215}{x^*}$$

$$c(T, x^*) = 0.000154084 - 0.0280301\,T + 0.00154587\,T^2 - 4.52701\cdot10^{-6}\,T^3 + \frac{0.0915323}{x^{*2}} + \frac{0.0711652}{x^*}$$

$$d(T, x^*) = -0.00509267 - 0.00796846\,T + 0.0000446828\,T^2 - 8.79425\cdot10^{-8}\,T^3 + \frac{0.133991}{x^{*2}} + \frac{0.831112}{x^*}$$

$$e(T, x^*) = -0.0227223 - 1.56512\,T + 0.00380717\,T^2 + 0.0000164109\,T^3 + \frac{1.29499}{x^{*2}} + \frac{0.0474821}{x^*}$$

$$f(T, x^*) = 0.00310646 + 0.304518\ T - 0.000564012\ T^2 - 2.03267\cdot10^{-6}\ T^3 - \frac{0.351584}{x^{*2}} + \frac{0.103749}{x^*}$$

$$g(T, x^*) = 0.077543 - 0.00196315\ T - 0.0000130412\ T^2 + 6.62369\cdot10^{-8}\ T^3 + \frac{0.011347}{x^{*2}} + \frac{0.0972804}{x^*}$$

$$h(T, x^*) = -0.153143 + 0.0575392\ T - 0.000306511\ T^2 - 2.96097\cdot10^{-8}\ T^3 - \frac{0.0982514}{x^{*2}} + \frac{0.336286}{x^*}$$

$$i(T, x^*) = -0.552173 - 0.00207043\ T + 0.0000144032\ T^2 + 8.83\cdot10^{-9}\ T^3 + \frac{0.0119833}{x^{*2}} - \frac{0.0700025}{x^*}$$

$$j(T, x^*) = 0.126544 - 0.00136029\ T + 5.90598\cdot10^{-6}\ T^2 - 4.1715\cdot10^{-9}\ T^3 + \frac{0.00170807}{x^{*2}} - \frac{0.0064323}{x^*}$$

The total number of molecules in the critical cluster N^*_{tot} is given by

$$N^*_{tot} = \exp[A(T, x^*) + B(T, x^*)\ln(RH/100) + C(T, x^*)\ln(RH/100)^2 + D(T, x^*)\ln(RH/100)^3 + E(T, x^*)\ln(N_a) + F(T, x^*)\ln(RH/100)\ln(N_a) + G(T, x^*)\ln(RH/100)^2\ln(N_a) + H(T, x^*)\ln(N_a)^2 + I(T, x^*)\ln(RH/100)\ln(N_a)^2 + J(T, x^*)\ln(N_a)^3] \quad (12)$$

where the coefficients $A(T, x^*)...I(T, x^*)$ again depend on temperature and critical cluster mole fraction x^* (from eq 10):

$$A(T, x^*) = 7.51024\cdot10^{-6} + 0.000502054\ T - 0.0000368602\ T^2 + 1.08256\cdot10^{-6}\ T^3 - \frac{0.000270282}{x^*}$$

$$B(T, x^*) = -4.30048\cdot10^{-6} - 0.000730133\ T + 0.000252062\ T^2 - 1.01648\cdot10^{-6}\ T^3 - \frac{0.00114283}{x^*}$$

$$C(T, x^*) = -4.42156\cdot10^{-6} - 0.0023486\ T + 3.0065\cdot10^{-7}\ T^2 + 2.44797\cdot10^{-8}\ T^3 - \frac{0.00250226}{x^*}$$

$$D(T, x^*) = -0.000167057 + 0.000207504\ T - 1.13013\cdot10^{-6}\ T^2 + 1.80268\cdot10^{-9}\ T^3 - \frac{0.0168245}{x^*}$$

$$E(T, x^*) = 0.0000985954 + 0.00451285\ T - 0.0000512557\ T^2 + 4.60749\cdot10^{-8}\ T^3 - \frac{0.00214318}{x^*}$$

$$F(T, x^*) = 0.0000636528 - 0.00288529\ T + 6.51706\cdot10^{-6}\ T^2 + 2.32601\cdot10^{-8}\ T^3 - \frac{0.0110319}{x^*}$$

$$G(T, x^*) = 0.000449239 + 0.0000689416\ T - 3.50302\cdot10^{-7}\ T^2 + 1.07451\cdot10^{-10}\ T^3 + \frac{0.00169646}{x^*}$$

$$H(T, x^*) = 0.000831844 - 5.35108\cdot10^{-6}\ T + 1.66432\cdot10^{-6}\ T^2 - 3.05108\cdot10^{-9}\ T^3 - \frac{0.000306251}{x^*}$$

$$I(T, x^*) = 0.00355374 + 0.0000306009\ T - 2.11004\cdot10^{-7}\ T^2 - 2.11436\cdot10^{-11}\ T^3 + \frac{0.00074989}{x^*}$$

$$J(T, x^*) = -0.00143534 + 7.856\cdot10^{-6}\ T - 3.45128\cdot10^{-8}\ T^2 + 5.21547\cdot10^{-11}\ T^3 - \frac{0.000021423}{x^*}$$

The radius on the cluster in nanometers is given as a function of the mole fraction and the total number of molecules in the cluster:

$$r^*[nm] = \exp[-1.6525507 + 0.45852848x^* + 0.33483673\ln(N^*_{tot})] \quad (13)$$

Table 1 summarizes the validity region of our parametrizations and their accuracy. The nucleation rate parametrization is least accurate for nucleation rates lower than $1/(cm^3s)$: if we confine ourselves to the region where the parametrization gives nucleation rates between $1/(cm^3s)$ and 10^{14} $/(cm^3s)$ it reproduces the model results within 1 order of magnitude ($0.1 < J_{theor}/J_{para} < 10$).

The threshold concentrations ($1/cm^3$) of sulfuric acid (total) that produce the nucleation rates $J = 1/(cm^3s)$ and $J = 10^6/(cm^3s)$ depend on temperature and relative humidity according to the following equations:

$$N_a^{J=1}[1/cm^3] = \exp\left[-2.51369 + 0.105916\ RH - \frac{2782.56}{T} - \frac{9.37597\ RH}{T} + 0.142594\ T - 0.000280101\ RH\ T - 0.0000941073\ T^2 - 10.7831\ln\left(\frac{RH}{100}\right) + \frac{1530.91\ln\left(\frac{RH}{100}\right)}{T} + 0.0159638\ T\ln\left(\frac{RH}{100}\right)\right] \quad (14)$$

$$N_a^{J=10^6}[1/cm^3] = \exp\left[-32.7828 + 0.0922094\ RH + \frac{1973.4}{T} - \frac{6.92952\ RH}{T} + 0.213356\ T - 0.000246469\ RH\ T - 0.000154046\ T^2 - 10.5619\ln\left(\frac{RH}{100}\right) + \frac{1579.88\ln\left(\frac{RH}{100}\right)}{T} + 0.0150701\ T\ln\left(\frac{RH}{100}\right)\right] \quad (15)$$

Figure 2 show the overall quality of the present parametrization. The ratio of theoretical and parametrized nucleation rates is between 0.1 and 10, excluding the very small nucleation rates below $1/(cm^3s)$ for which the accuracy is somewhat poorer.

Nucleation Rates. Figure 3a,b shows the threshold sulfuric acid concentrations needed to produce a nucleation rate of 1 and 10^6 $1/(cm^3s)$, respectively, as functions of relative humidity. The results are shown using different temperatures, from 300.15 to 400.15 K in 10 K intervals. The symbols show the results of the rigorous calculation, the lines the values given by the parametrization. This type of figure is valuable in identifying the regions in parameter space in which nucleation can occur. In atmospheric conditions, it is typical

TABLE 1: Summary of the Validity Regions of Our Model, the Range of Results, and Accuracy of the Parametrization

$300.15\ \mathrm{K} \le T \le 400.15\ \mathrm{K}$	
$2 \cdot 10^9/\ \mathrm{cm}^3 \le N_a \le 2 \cdot 10^{15}/\ \mathrm{cm}^3$	
$1\% \le \mathrm{RH} \le 100\%$	
$10^{-1} < J/(\mathrm{cm}^3\mathrm{s}) < 10^{14}$	$0.02 < J_{theor}/J_{para} < 11$
$0.15 < x^* < 0.54$	$-0.007 < x^*_{theor} - x^*_{para} < 0.006$
$6 < N^*_{tot} < 133$	$-1.4 < N^*_{tot,\,theor} - N^*_{tot,\,para} < 3.1$
$0.4 < r^* < 1.16$	$-0.011 < r^*_{theor} - r^*_{para}\ (\mathrm{nm}) < 0.018$

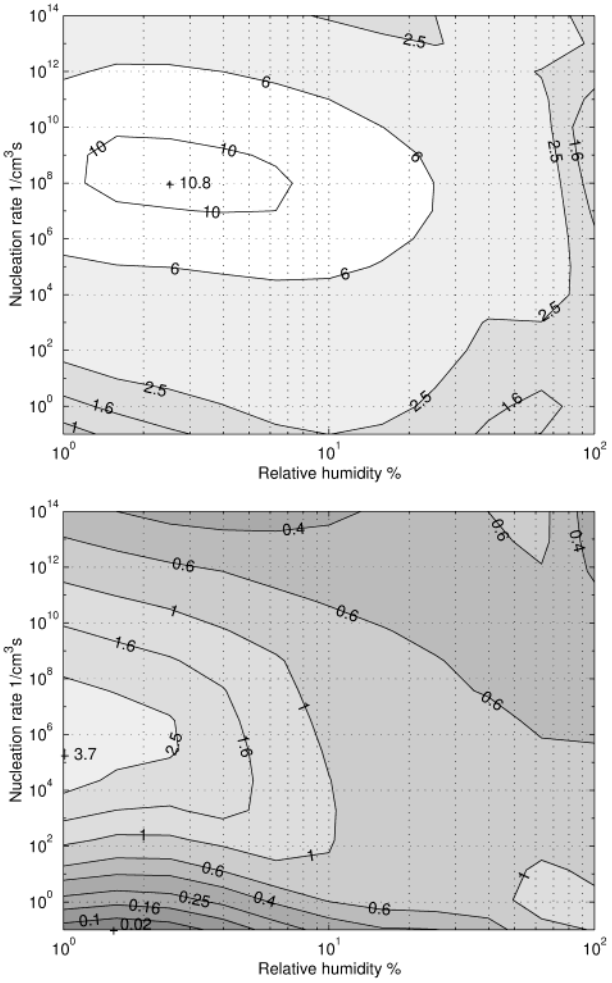

FIGURE 2. Comparison between the theoretical and parametrized nucleation rates: the contour plots show (a) the maximum and (b) the minimum value of the ratio J_{theor}/J_{param} over the whole temperature range.

to choose a nucleation rate of unity to represent the set off limit. However, in cases such as cooling of exhaust the concentration of sulfuric acid molecules as well as the nucleation rate may be significantly higher—thus it was also chosen to show the parameter combinations resulting in a rate of 10^6 1/(cm^{3}s). The agreement between the nucleation rates calculated using the full model and parametrized one can also been seen.

In Figure 4 the new model (and new parametrization) for threshold concentrations of sulfuric acid were compared to two old parametrizations (*6*, *39*) at 300 K, where all these models are valid. The present model and the parametrization by Kulmala et al. (*6*) have a reasonable agreement, only the dependence of relative humidity is different. The parametrization of Wexler et al. (*39*) gives somewhat lower threshold concentrations (higher nucleation rates for fixed conditions).

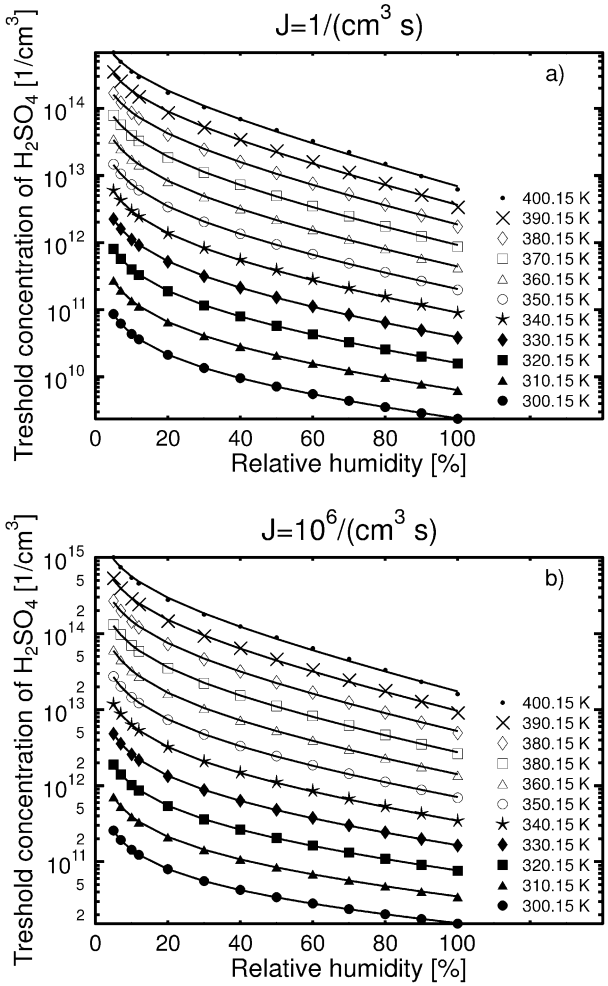

FIGURE 3. Comparison between the parametrization (lines) and the theoretical values (symbols) for the threshold sulfuric acid concentration required for nucleation rate (a) $J = 1/(\mathrm{cm}^3\mathrm{s})$ and (b) $J = 10^6/(\mathrm{cm}^3\mathrm{s})$.

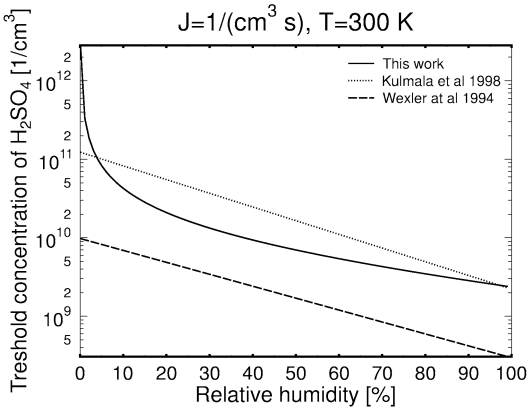

FIGURE 4. Comparison between the different parametrizations for the threshold sulfuric acid concentration required for nucleation rate $J = 1/(\mathrm{cm}^3\mathrm{s})$.

Figures 5−7 show nucleation rates as functions of different ambient parameters (temperature, relative humidity, sulfuric acid concentration). The rates are calculated using the parametrization. In Figure 5 the nucleation rate is shown as a function of sulfuric acid concentration for nine different sets of conditions regarding temperature (300 K, 350 K, 400 K) and relative humidity (1%, 10%, 100%).

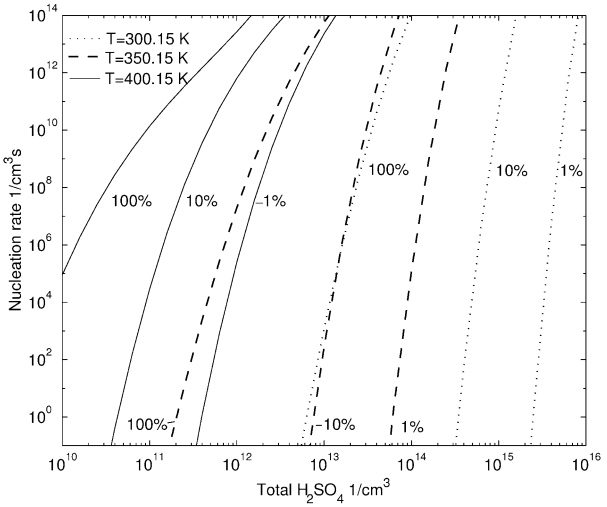

FIGURE 5. Nucleation rate as a function of sulfuric acid concentration. Different line types represent different temperatures and relative humidities are marked by the curves.

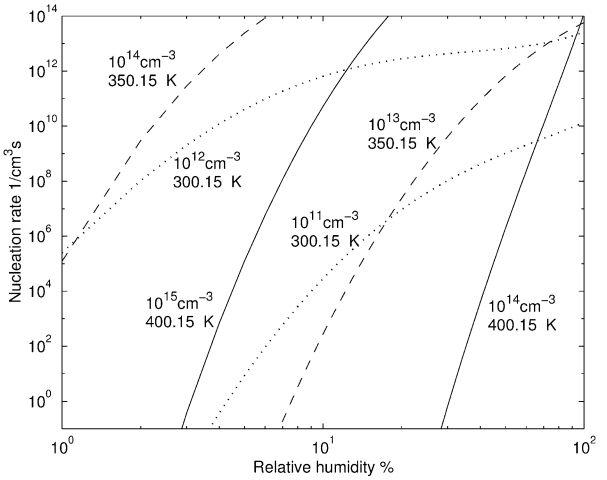

FIGURE 6. Nucleation rate as a function of relative humidity. Different line types represent different temperatures and sulfuric acid concentrations are marked by the curves.

The figure shows that the nucleation rate is an extremely sensitive function of the sulfuric acid concentration. Indeed, a factor of 10 change in the sulfuric acid concentration can lead to a 10 orders of magnitude change in nucleation rate. In Figure 6, the nucleation rate is shown as a function of relative humidity for six different sets of conditions regarding temperature and sulfuric acid concentration (300 K − 10^{11} 1/cm^3, 300 K − 10^{12} 1/cm^3, 350 K − 10^{13} 1/cm^3, 350 K − 10^{14} 1/cm^3, 400 K − 10^{14} 1/cm^3, 400 K − 10^{15} 1/cm^3).

It is evident that the dependence on relative humidity is much more sensitive at higher temperatures. In Figure 7, the nucleation rate is shown as a function of temperature for nine different sets of conditions regarding sulfuric acid concentration (10^{12}, 10^{13}, and 10^{14} 1/cm^3) and relative humidity (1%, 10%, 100%). Now, a high value for sulfuric acid concentration means a greater sensitivity on temperature.

In Figure 8 the nucleation rates given by the present and some other recent parametrizations are compared, as functions of temperature for three different sets of conditions for relative humidity and sulfuric acid concentration (50% − 10^{11} 1/cm^3, 50% − 10^{12} 1/cm^3, 100% − 10^{11} 1/cm^3). There are several interesting aspects of the figure. First of all, it must be noted that the old parametrization (*6*) and the new low-temperature parametrization (*33*) are strictly valid only up

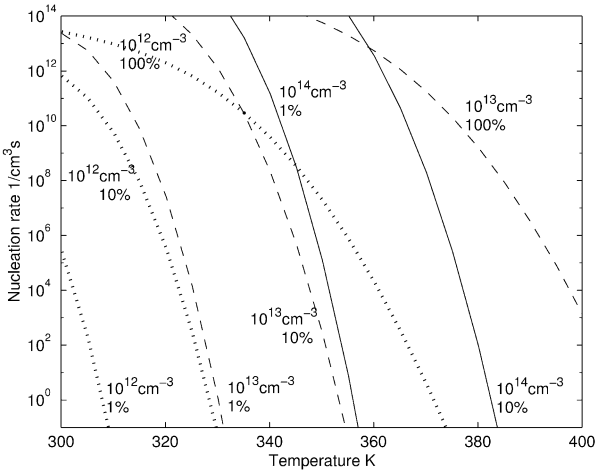

FIGURE 7. Nucleation rate as a function of temperature. Different line types represent different sulfuric acid concentrations and relative humidities are marked by the curves.

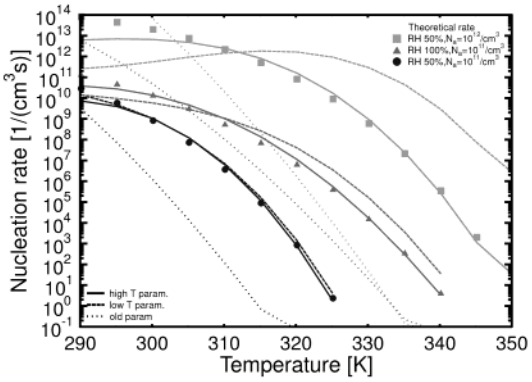

FIGURE 8. Theoretical nucleation rate and different parametrizations as a function of temperature.

to 300 K. Thus their predictions must be treated only as extrapolations of the model results. However, since such extrapolative techniques seem to have been used in diesel exhaust simulations, we think it is of importance to discuss model performance at these high temperatures. First of all, at high temperatures (320 K − 350 K) the extrapolated new low temperature parametrization seems to give higher nucleation rates that the present high temperature parametrization. The extrapolation, however, seems to behave badly at these high temperatures. This is clear from the 50% − 10^{12} 1/cm^3 curve. It is unphysical for the nucleation rate to increase as a function of temperature, when the relative humidity and sulfuric acid concentrations are kept constant. The reason for this ill behavior is the use of polynomials in the parametrizations and emphasis that it is crucial not to use the parametrizations outside their documented applicability range. Another important issue is the too low estimates of the old parametrization at high temperatures. This parametrization was used by Shi and Harrison (*5*) to model diesel exhaust dilution. They found that the observed nucleation rate was several orders of magnitude higher that that given by the parametrization. The new high-temperature parametrization might thus work better to describe their experiments. The recent comparisons between binary and ternary nucleation rates indicate that a small amount of ammonia will increase the nucleation rate significantly. Our parametrization reduces computational time by a factor of at least 500, compared with a rigorous simulation of binary nucleation, and are thus convenient to use in large scale models, in which not much computational effort can be spent in any of the subprocesses.

Acknowledgments

This work was supported the by European Commission under the contract (EVK-2002, project PARTS) and Academy of Finland (Project No. 47668). The authors would like to thank Adam Foster for checking the manuscript for grammatical errors.

Literature Cited

(1) Dockery, D. W.; Pope, C. A. *Annu. Rev. Public. Health* **1994**, *15*, 107−132.
(2) *Proposed identification of diesel exhaust as a toxic air contaminant, part b: Health risk assessment for diesel exhaust*; California Environme, 1998.
(3) *Diesel Exhaust*: *A Critical Analysis of Emissions, Exposure and Health Effects*; Health Effects Institute: Cambridge, MA, 1995.
(4) *Diesel Emissions and Lung Cancer*: *Epidemiology and Quantitative Risk Assessment*; Health Effects Institute: Cambridge, MA, 1999.
(5) Si, J. P.; Harrison, R. M. *Environ. Sci. Technol.* **1999**, *33*, 3730−3736.
(6) Kulmala, M.; Laaksonen, A.; Pirjola, L. *J. Geophys. Res.* **1998**, *103*, 8301−8308.
(7) Abdul-Khalek, I.; Kittelson, D. B.; Brear, F. *The influence on dilution conditions on diesel exhaust particle size distribution measurements*; Technical Report 1999-01-1142; Society of Automotiv, 1999.
(8) Abdul-Khalek, I.; Kittelson, D. B.; Brear, F. *Nanoparticle growth during dilution and cooling of diesel exhaust: experimental investigation and theoretical assesment*; Technical Report 2000-01-0515; Society of Automotiv, 2000.
(9) Tobias, H. J.; Beving, D. E.; Ziemann, P. J.; Sakurai, H.; Zuk, M.; McMurry, P. H.; Zarling, D.; Waytulonis, R.; Kittelson, D. B. *Environ. Sci. Technol.* **2001**, *35*, 2233−2243.
(10) Weber, R. J.; McMurry, P. H.; Mauldin, L.; Tanner, D. J.; Eisele, F. L.; Brechtel, F. J.; Kreidenweis, S. M.; Kok, G. L.; Schilawski, R. D.; Baumgardner, D. *J. Geophys. Res.* **1998**, *103*, 16,385−16,-396.
(11) Clarke, A. D.; Varner, J. L.; Eisele, F.; Mauldin, R. L.; Tanner, D.; Litchy, M. *J. Geophys. Res.* **1998**, *103*, 16, 397−16, 409.
(12) Kulmala, M.; Hämeri, K.; Aalto, P.; Mäkelä, J.; Pirjola, L.; Nilsson, E. D.; Buzorius, G.; Rannik, Ü.; Dal Maso, M.; Seidl, W.; Hoffmann, T.; Jansson, R.; Hansson, H.-C.; O'Dowd, C.; Viisanen *Tellus B* **2001**, *53*, 324−343.
(13) Noppel, M.; Vehkamäki, H.; Kulmala, M. *J. Chem. Phys.* **2002**, *116*, 218−228.
(14) McGraw, R.; Weber, R. J. *Geophys. Res. Lett.* **1998**, *25*, 3143−3146.
(15) Hanson, D. R.; Eisele, F. *J. Phys. Chem.* **2000**, *104*, 1715−1719.
(16) Re, S.; Osamura, Y.; Morokuma, K. *J. Phys. Chem.* **1999**, *A103*, 3535−3547.
(17) Alberty, R. A. *Physical chemistry*; John Wiley & Sons: New York, 6th ed.; 1983.
(18) Jaecker-Voirol, A.; Mirabel, P.; Reiss, H. *J. Chem. Phys.* **1987**, *87*, 4849−4852.
(19) Noppel, M. *J. Chem. Phys.* **1998**, *109*, 9052−9056.
(20) Trinkaus, H. *Phys. Rev. B* **1983**, *27*, 7372−7378.
(21) Arstila, H.; Korhonen, P.; Kulmala, M. *J. Aerosol Sci.* **1999**, *30*, 131−138.
(22) Wilemski, G.; Wyslouzil, B. E. *J. Chem. Phys.* **1995**, *103*, 1127−1136.
(23) Preining, O.; Wagner, P. E.; Pohl, F. G.; Szymanski, W. *Heterogeneous Nucleation and Droplet Growth*; University of Vienna, Institute of Experimental Physics: Vienna, Austria, 1981.
(24) Ayers, G. P.; Gillett, R. W.; Gras, J. L. *Geophys. Res. Lett.* **1980**, *7*, 433−436.
(25) Kulmala, M.; Laaksonen, A. *J. Chem. Phys.* **1990**, *93*, 696−701.
(26) Sabinina, L.; Terpugow, L. *Z. Phys. Chem.* **1935**, *A173*, 237−241.
(27) Morgan, L. J.; Davies, C. E. *J. Am. Chem. Soc.* **1916**, *28*, 555−568.
(28) Suggitt, R. M.; Aziz, P. M.; Wetmor, F. E. W. *J. Am. Chem. Soc.* **1949**, *71*, 676−678.
(29) Hoffmann, W.; Seeman, F. W. *Z. Physik. Chem. Neue Folge* **1960**, *24*, 300−306.
(30) Myhre, C. E. L.; Nielsen, C. J.; Saastad, O. W. *J. Chem. Eng. Data* **1998**, *43*, 617−622.
(31) Vargaftik, N. B.; Volkov, B. N.; Voljak, L. D. *J. Phys. Chem. Ref. Data* **1983**, *12*, 817−820.
(32) Reid, R. C.; Prausnitz, J. M.; Poling, P. E. *The properties of gases and liquids*; McGraw-Hill: New York, 1987.
(33) Vehkamäki, H.; Kulmala, M.; Napari, I.; Lehtinen, K. E. J.; Timmreck, C.; Noppel, M.; Laaksonen, A. *J. Geophys. Res.* **2002**, *107*, 4622.
(34) *International Critical Tables of Numerical Data Physics, Chemistry and Technology*; McGraw-Hill: New York, 1928; Vol. I, pp 56−57.
(35) Taleb, D.-E.; Ponche, J.-L.; Mirabel, P. *J. Geophys. Res.* **1996**, *101*, 25967−25977.
(36) Clegg, S. L.; Brimblecombe, P.; Wexler, A. S. *J. Phys. Chem.* **1998**, *102*, 2A, 2137−2154.
(37) Clegg, S. L.; Brimblecombe, P. *J. Chem. Eng. Data* **1995**, *40*, 43−64.
(38) Zeleznik, F. J. *J. Phys. Chem. Ref. Data* **1991**, *20*, 1157−1200.
(39) Wexler, A. S.; Lurmann, F. W.; Seinfeld, J. H. *Atmos. Environ.* **1994**, *28*, 531−546.

Received for review November 19, 2002. Revised manuscript received March 26, 2003. Accepted March 31, 2003.

ES0263442